

Research Article

An Investigation of Acoustic Attenuation Performance of Silencers with Mean Flow Based on Three-Dimensional Numerical Simulation

Wei Fan and Li-Xin Guo

School of Mechanical Engineering and Automation, Northeastern University, Shenyang 110819, China

Correspondence should be addressed to Li-Xin Guo; lxguo@mail.neu.edu.cn

Received 28 June 2015; Revised 18 September 2015; Accepted 27 September 2015

Academic Editor: M. I. Herreros

Copyright © 2016 W. Fan and L.-X. Guo. This is an open access article distributed under the Creative Commons Attribution License, which permits unrestricted use, distribution, and reproduction in any medium, provided the original work is properly cited.

Transmission loss (TL) is often used to evaluate the acoustic attenuation performance of a silencer. In this work, a three-dimensional (3D) finite element method (FEM) is employed to calculate the TL of some representative silencers, namely, circular expansion chamber silencer and straight-through perforated pipe silencer. In order to account for the effect of mean flow that exists inside the silencer, the 3D FEM is used in conjunction with the Computational Fluid Dynamics (CFD) simulation of the flow field. More concretely, the 3D mean flow field is computed by firstly using CFD, and then the obtained mean flow data are imported to an acoustic solution undertaken using FEM. The data transfer between the two steps is accomplished by mesh mapping. The results presented demonstrate good agreement between present TL predictions and previously published experimental and numerical works. Also, the details of the flow inside the silencers may be studied. Furthermore, the effect of mean flow velocity on acoustic attenuation performance of the silencers is investigated. It is concluded that for the studied silencers, in general, increasing flow velocity increases the TL and decreases the resonance peaks.

1. Introduction

It is common for silencing devices to be used to attenuate exhaust noise generated by vehicles and various fluid machines. It is well known that the silencer is always accompanied with mean gas flow in practical application. Many studies, including theoretical and experimental methods, had been conducted to investigate the acoustic attenuation performance of the silencer with mean flow during the past years [1–5]. With the rapid development of high-performance computers, recent years have seen an increasing interest in adopting 3D numerical methods to predict silencer performance. Generally speaking, two kinds of numerical methods are available, namely, time-domain method [6–8] based on the nonlinear fluid dynamic model and frequency-domain method based on the linear acoustic model. The frequency-domain method mainly includes boundary element method (BEM) [9–11] and finite element method (FEM).

FEM was initially applied to predict the acoustic performance of mufflers by Young and Crocker [12]. Due to

restrictions in computational resources, most of previously published applications of FEM had been limited to two-dimensional analyses with simplified boundary conditions. However, realistic silencer geometries often exhibit 3D features; hence these analyses tend to be less accurate when dealing with complex geometries. As mentioned before, with the ever-increasing computational speed and memory capacity of the computer in recent years, more applications of 3D FEM can be found in the literature. For example, Mehdizadeh and Paraschivou [13] implemented a comprehensive 3D FEM to assess TL of a packed muffler and a parallel baffle silencer with nonhomogeneous domain in the absence of mean flow, and the success of the 3D finite element modeling encouraged extending the application of the FEM to more complex cases. Kang and Ji [14] adopted 3D FEM to study the acoustic length correction of duct extension into a cylindrical chamber and examined the effect of chamber geometry on the acoustic length correction. Ge et al. [15] applied 3D FEM to predict the acoustic attenuation characteristics of complex perforated

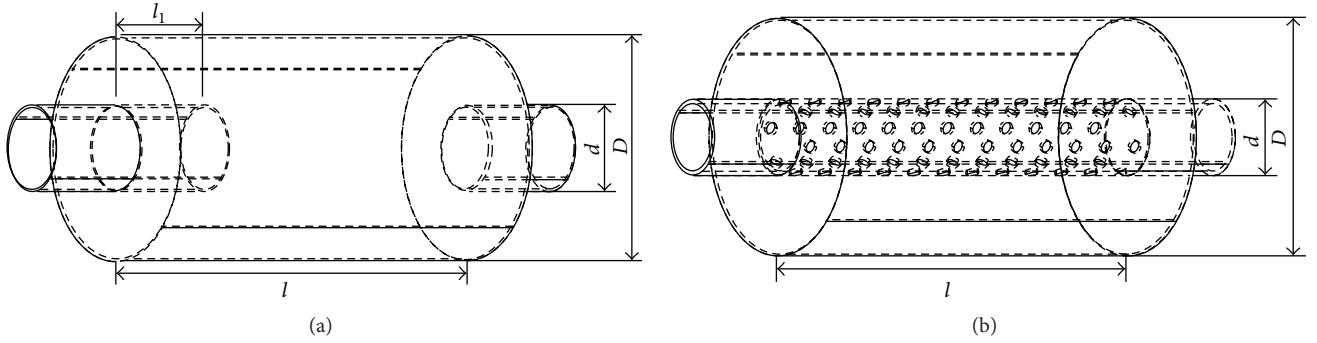


FIGURE 1: Geometries of the silencers considered: (a) circle expansion chamber silencer and (b) straight-through perforated pipe silencer.

pipe silencers with the help of perforate impedance models. Furthermore, the effects of perforation length and porosity on the acoustic performance are investigated. Chaitanya and Munjal [16] used 3D FEM analysis to investigate the effect of wall thickness of the inlet/outlet duct on end correction, and their predictions are validated by comparing them with experimental data. In order to improve the acoustic attenuation performance of an exhaust muffler in 175 series of agriculture diesel engine, Fu et al. [17] established a 3D model for the muffler and then employed commercial finite element software package to calculate the TL, and their predictions showed very close agreement with experimental data.

In the aforementioned works, the applications of FEM mainly focus on predicting TL in silencers without mean flow. Of course, FEM is capable of considering the effect of mean flow by assuming that the acoustic field is superimposed over the decoupled mean flow, but this mean flow must be imported from an external steady flow computation that is often performed by a simplified potential-flow approach [18, 19] in previous works. In this paper, to acquire a more realistic flow distribution inside the silencer, the CFD simulation with proper turbulence model, which is extremely useful in determining the flow distribution and commonly used for analyzing the mean flow performance [6, 8, 20–22], is utilized to perform the external steady flow computation via commercial software ANSYS FLUENT 14.5. After finishing the CFD computation, the mean flow data are used as an input into the acoustic field, and then an acoustic response analysis is carried out using FEM via commercial software LMS Virtual.Lab 11.0. Finally, the TL with the effect of mean flow is calculated.

2. Method

2.1. Silencer Modeling. In present work, the circle expansion chamber silencer with extended inlet used in [23] and three straight-through perforated pipe silencers used in [24] are considered. Also, the published experimental data from these authors are used as a basis for comparison of the numerical results presented in this paper. Figure 1 shows the 3D geometries of the silencers considered here and their precise dimensions are given in Table 1, where d_h and σ denote the diameter of the orifice on the perforated pipe and the porosity, respectively.

TABLE 1: Dimensions for the silencers considered (unit: mm).

| Silencer | D | d | l | l_1 | d_h | σ (%) |
|-----------------------------|-----|-----|-----|-------|-------|--------------|
| Expansion chamber | 108 | 40 | 208 | 52 | — | — |
| Perforated pipe 1 (P_1) | 110 | 32 | 200 | — | 4 | 4.7 |
| Perforated pipe 2 (P_2) | 110 | 32 | 200 | — | 6 | 9.0 |
| Perforated pipe 3 (P_3) | 110 | 32 | 200 | — | 8 | 14.7 |

Tetrahedral mesh is chosen to discretize the computational field of the silencer due to its high flexibility. Two different meshes, namely, CFD mesh and acoustic mesh, will be used for the solution of mean flow and acoustic problems, respectively. For the expansion chamber silencer, the element sizes of CFD and acoustic meshes are 4 mm and 8 mm, respectively, and the CFD mesh is composed of 131111 nodes and 406204 elements; the acoustic mesh is composed of 51972 nodes and 35807 elements. For the straight-through perforated pipe silencer whose geometry is relatively complex, the computational model is split into several parts to generate mesh individually in order to decrease computational cost. An element size of 2 mm is used for the perforation area in both CFD and acoustic meshes, and the element sizes for the rest of the two meshes are 4 mm and 10 mm, respectively. Take silencer P_2 as an example; the CFD mesh is composed of 206827 nodes and 1142767 elements; the acoustic mesh is composed of 668038 nodes and 479644 elements.

Figures 2(a) and 3(a) show the generated CFD mesh, which is fine and dense, and the mesh near to the walls is densified further in order to resolve the boundary layer. Compared with the CFD mesh, the acoustic mesh shown in Figures 2(b) and 3(b) is coarse and thin. But it should be noted that, to ensure computational accuracy, the maximum size of the acoustic mesh must meet the following formulation [25]:

$$L \leq \frac{c}{6f_{\max}}, \quad (1)$$

where c is the speed of sound and f_{\max} is the maximum frequency of interest. The maximum achieved frequency of acoustic mesh can be calculated directly in Virtual.Lab, and it is found that the maximum achieved frequencies of generated acoustic meshes for the studied silencers are all

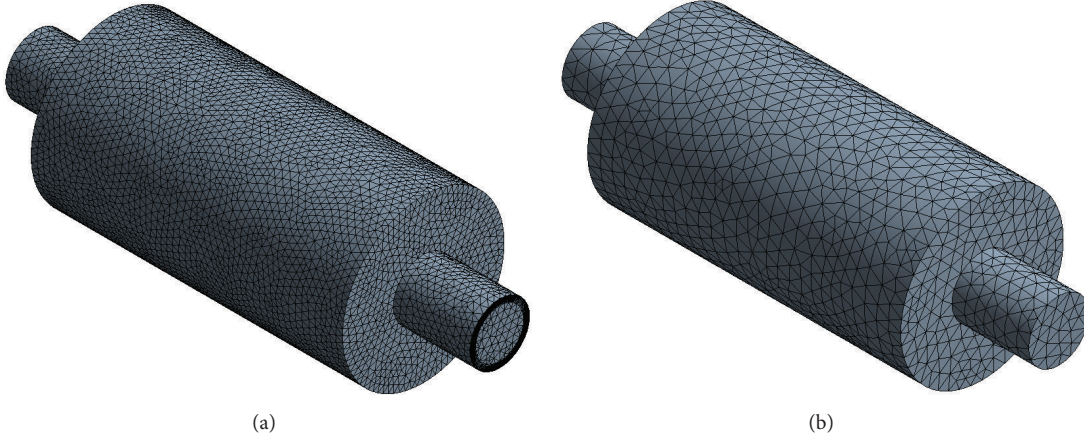


FIGURE 2: Geometry of meshes for the expansion chamber silencer: (a) CFD mesh and (b) acoustic mesh.

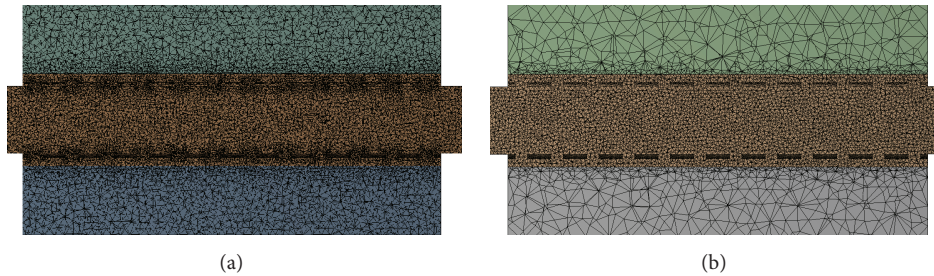


FIGURE 3: Geometry of meshes for the straight-through perforated pipe silencer: (a) CFD mesh and (b) acoustic mesh.

above 3500 Hz, well over the maximum frequency of interest (3000 Hz). Therefore, the accuracy of acoustic computation can be ensured.

2.2. Prediction of TL. In the CFD steady flow computation, the data type used is double precision, the solver implemented is a pressure-based implicit solver, SIMPLEC pressure-velocity coupling algorithm is chosen with second-order scheme for spatial discretisation, and the realizable k -epsilon turbulence model is employed [26]. The fluid material is air with the density conforming to the ideal gas law. The boundary conditions consist of the following: (i) a mass-flow-inlet with constant mass flux, (ii) a pressure-outlet with constant static pressure, in this case 0 Pa relative to one standard atmospheric pressure, and (iii) a series of walls assumed to be stationary, with no slip, and adiabatic. After convergence of the CFD computation, the flow velocity data are exported into format CGNS (CFD General Notation System) and then imported to the acoustic field to serve as a mean flow boundary condition of the acoustic response analysis (i.e., the mean flow field is superimposed over the acoustic field). Note that the purpose of using this CFD simulation is to obtain a more realistic and detailed flow velocity distribution inside the silencers, rather than to consider the viscous effect of mean flow on sound propagation as the full time-domain CFD method [7, 8] conducts.

The data transfer between acoustic and mean flow problems is accomplished by mesh mapping function that Virtual.Lab provides. Because there is no one-to-one correspondence between nodes of generated CFD and acoustic meshes, an appropriate mapping algorithm should be employed. In this paper, *Maximum Distance Algorithm* [27], which is often applied to set a mesh mapping between two meshes with different density of nodes, is employed, and this algorithm includes two necessary parameters: (i) *number of nodes* (N): it is the maximum number of nodes from the source mesh (CFD mesh) that is considered for mapping with one node of the target mesh (acoustic mesh) and (ii) *maximum distance* (R): only the nodes of the source mesh lying inside a sphere with radius R , centered at the node of target mesh, are taken into account. N closest to a given source node are used to transfer data to the target node. The data value assigned to the target node is a weighted average of the value at the N source nodes. The weights are [27]

$$W_i = \frac{1/d_i}{\sum_{i=1}^N (1/d_i)}. \quad (2)$$

The transferred value on the target node is then

$$v_{\text{Target}} = \frac{\sum_{i=1}^N (v_i^{\text{Source}}/d_i)}{\sum_{i=1}^N (1/d_i)}, \quad (3)$$

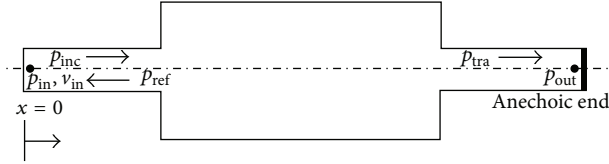


FIGURE 4: Theory for TL calculation.

where d_i is the distance between source node and target node and v^{Source} is the value of source node. The N and R could be given automatically when CFD and acoustic meshes are introduced to the data transfer module in Virtual.Lab; here we calculate directly using the defaults.

After finishing the data transfer, the acoustic response analysis is performed with 10 Hz spacing using FEM. For the sound field inside the silencer, the governing formulation is Helmholtz equation as [13]

$$\nabla^2 p + k^2 p = 0, \quad (4)$$

where p is the acoustic pressure, k is the wave number defined as $k = \omega/c$, ω is the angular frequency, and c is the speed of sound. Galerkin's method of weighted residuals is applied to (4) and the acoustic finite element formulation [28] is formed:

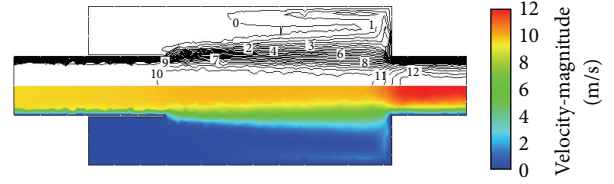
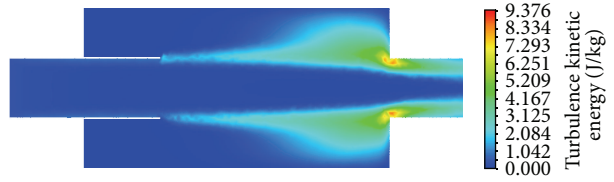
$$([M] - k^2 [P]) \{p\} = -j\rho\omega \{F\}, \quad (5)$$

where $[M]$ and $[P]$ are the inertia and stiffness matrices of the element, $\{p\}$ is the vector of acoustic pressure at all nodes of the system, ρ is the density of the medium, and $\{F\}$ is the forcing vector at all nodes of the system. At the inlet of the silencer a unit velocity of $u_{\text{in}} = 1$ m/s is imposed and the outlet is defined to be an anechoic end by setting an Anechoic End Duct Property in Virtual.Lab. In order to model the effect of mean flow on sound propagation, the mean flow boundary condition is set on the inlet [27]. Applying these boundary conditions and solving (5) may obtain the sound pressure at all nodes of the system. And, then, the TL is determined by [8]. Consider

$$\text{TL} = 20 \log_{10} \left[\left(\frac{A_{\text{in}}}{A_{\text{out}}} \right)^{1/2} \left| \frac{p_{\text{inc}}}{p_{\text{tra}}} \right| \right], \quad (6)$$

where A_{in} and A_{out} are the cross-sectional areas of the inlet and outlet of the silencer, respectively, p_{inc} is the acoustic pressure of incident wave at the inlet of the silencer, and p_{tra} is the acoustic pressure of transmitted wave at the outlet of the silencer. However, it should be pointed out that the results obtained using FEM are acoustic pressure at the inlet and outlet (p_{in} and p_{out}) which include the acoustic pressure of reflective wave (p_{ref}), as shown in Figure 4, where x represents the coordinate of the point along the silencer axis. Therefore, (6) should be further deduced to build the relationship between p_{in} , p_{out} and p_{inc} , p_{tra} .

In the frequency range of interest for silencer analysis, these acoustic pressure waves typically travel through the

FIGURE 5: Counters of velocity-magnitude for the expansion chamber silencer with inlet flow velocity of $v = 10.2$ m/s.FIGURE 6: Counters of turbulent kinetic energy for the expansion chamber silencer with inlet flow velocity of $v = 10.2$ m/s.

inlet and outlet pipes as plane waves [17]. When the wave travels in an inviscid moving medium, the 1D wave formulation is [29]

$$\frac{\partial^2 p}{\partial t^2} + 2V \frac{\partial^2 p}{\partial x \partial t} + (V^2 - c^2) \frac{\partial^2 p}{\partial x^2} = 0, \quad (7)$$

where V is the flow velocity of the medium. Solving (7) with the corresponding boundary and initial conditions in the time-domain gives p as a function of time and space [13]. By assuming a time-harmonic solution for the acoustic pressure (i.e., assuming that the time dependence takes an exponential form), (7) is solved to obtain the acoustic pressure at the inlet, which is written as

$$p_{\text{in}} = (p_{\text{inc}} e^{-jkx/(1+M)} + p_{\text{ref}} e^{+jkx/(1-M)}) e^{j\omega t}, \quad (8)$$

where p_{ref} is the acoustic pressure of reflective wave at the inlet and M is the mean flow Mach number defined as $V = M/c$. The particle velocity at the inlet also satisfies the same wave formulation, and one can write

$$u_{\text{in}} = \frac{1}{\rho c} (p_{\text{inc}} e^{-jkx/(1+M)} - p_{\text{ref}} e^{+jkx/(1-M)}) e^{j\omega t}, \quad (9)$$

where ρc represents the characteristic impedance of the medium at the inlet. As mentioned before, there are $x = 0$

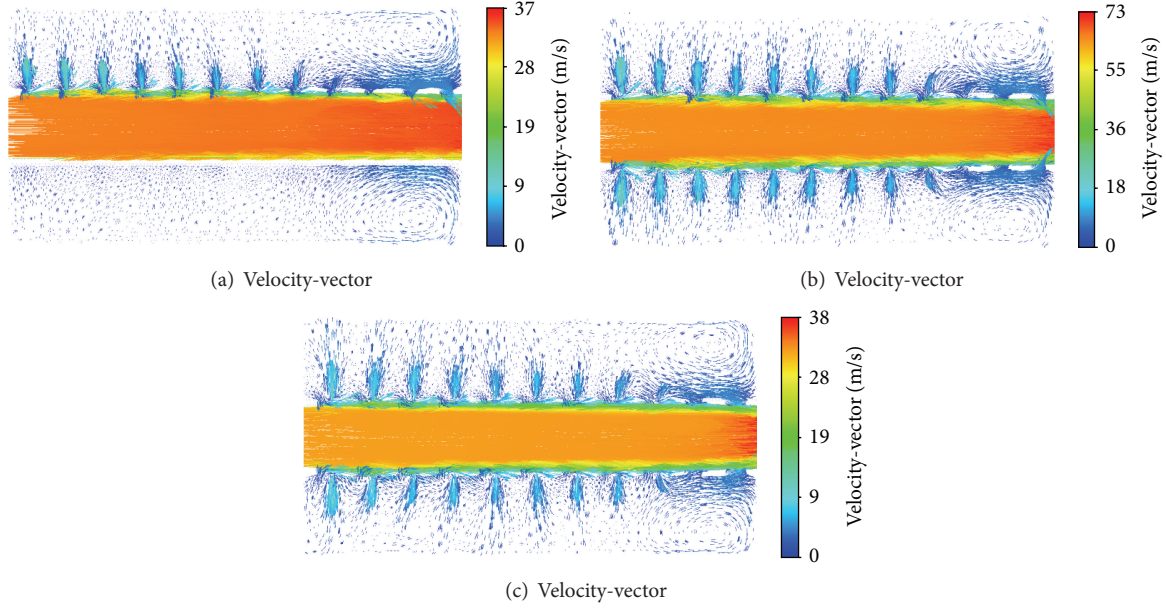


FIGURE 7: Velocity-vectors for the straight-through perforated pipe silencers: (a) silencer P_1 , $M = 0.1$, (b) silencer P_2 , $M = 0.2$, and (c) silencer P_3 , $M = 0.1$.

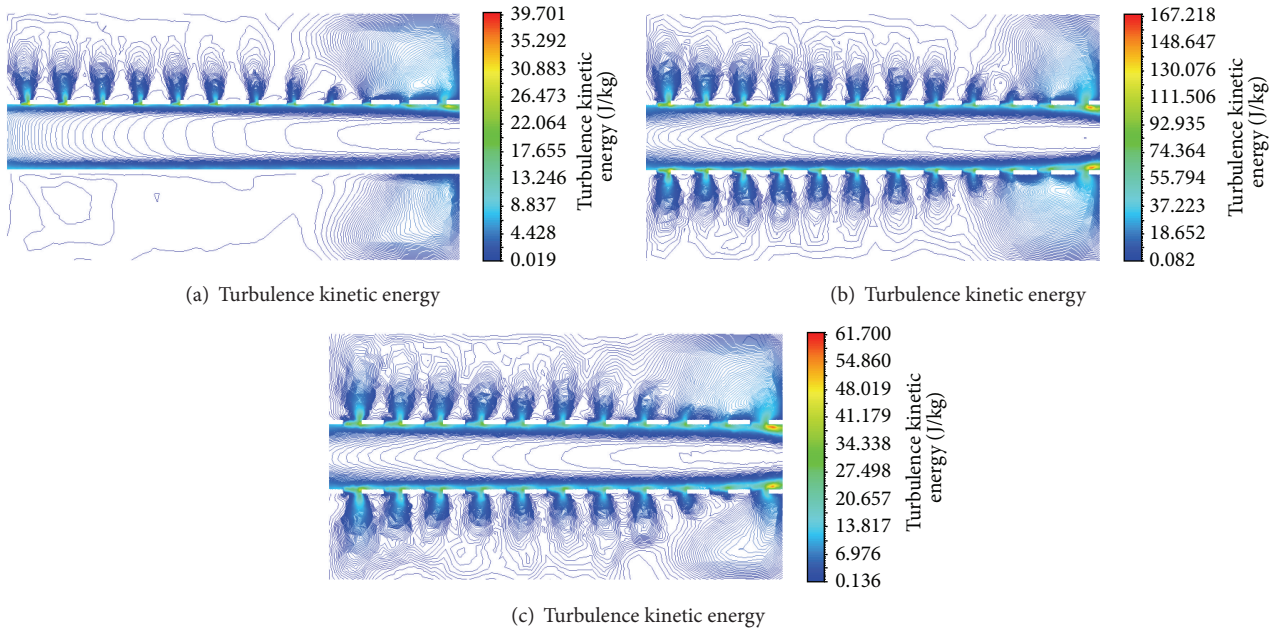


FIGURE 8: Counters of turbulent kinetic energy for the straight-through perforated pipe silencers: (a) silencer P_1 , $M = 0.1$, (b) silencer P_2 , $M = 0.2$, and (c) silencer P_3 , $M = 0.1$.

and $u_{in} = 1$ m/s at the inlet, and, with neglecting “ $e^{j\omega t}$ ” item, (8) and (9) reduce to

$$\begin{aligned} p_{in} &= p_{inc} + p_{ref}, \\ u_{in} &= \frac{1}{\rho c} (p_{inc} - p_{ref}) = 1 \end{aligned} \quad (10)$$

which yield

$$p_{inc} = \frac{p_{in} + \rho c}{2}. \quad (11)$$

In addition, the outlet is defined to be an anechoic end (i.e., the acoustic pressure of reflective wave at the outlet is 0), so there is

$$p_{tra} = p_{out}. \quad (12)$$

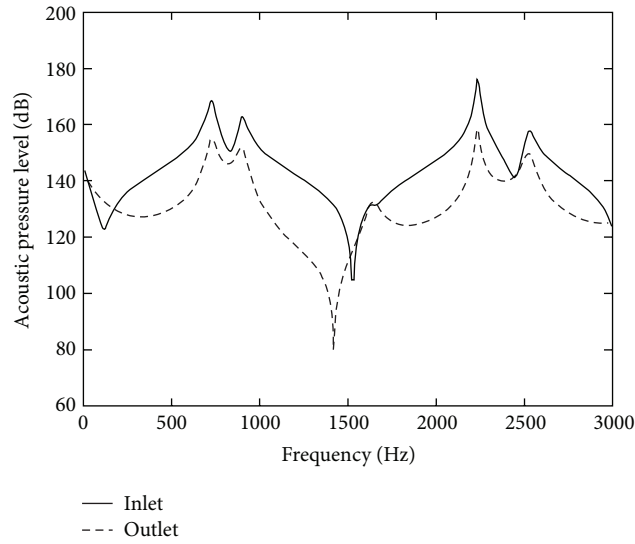
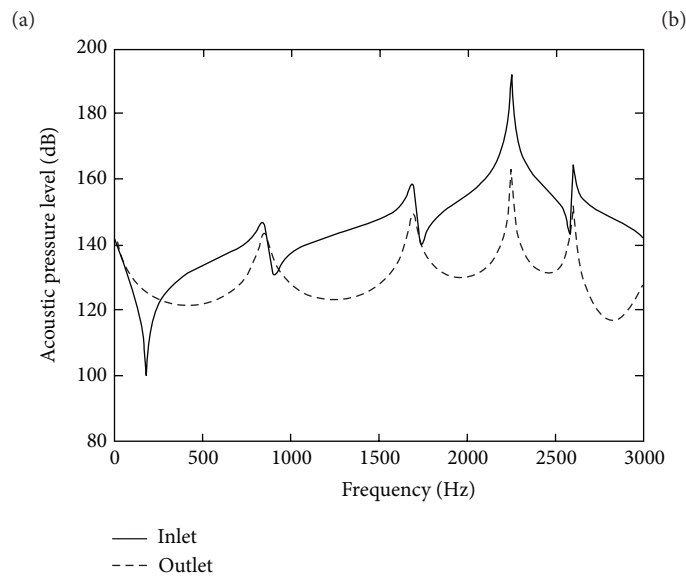
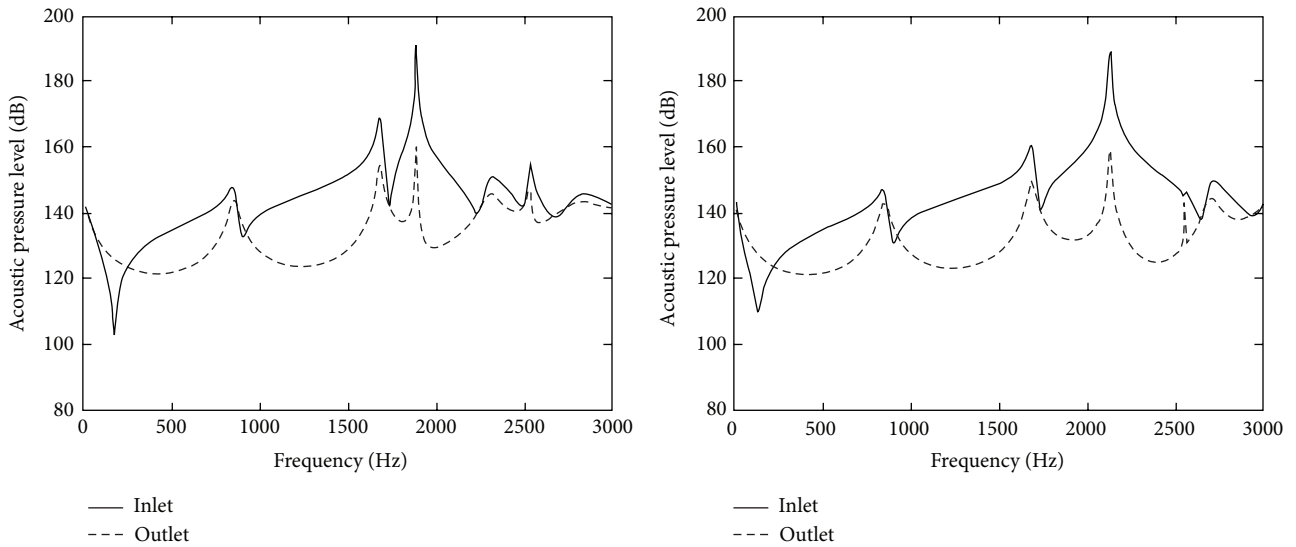


FIGURE 9: Acoustic pressure level for the inlet and outlet of the expansion chamber silencer with inlet flow velocity of $v = 10.2$ m/s.



(c)

FIGURE 10: Acoustic pressure level for the inlet and outlet of the straight-through perforated pipe silencers: (a) silencer P_1 , $M = 0.1$, (b) silencer P_2 , $M = 0.2$, and (c) silencer P_3 , $M = 0.1$.

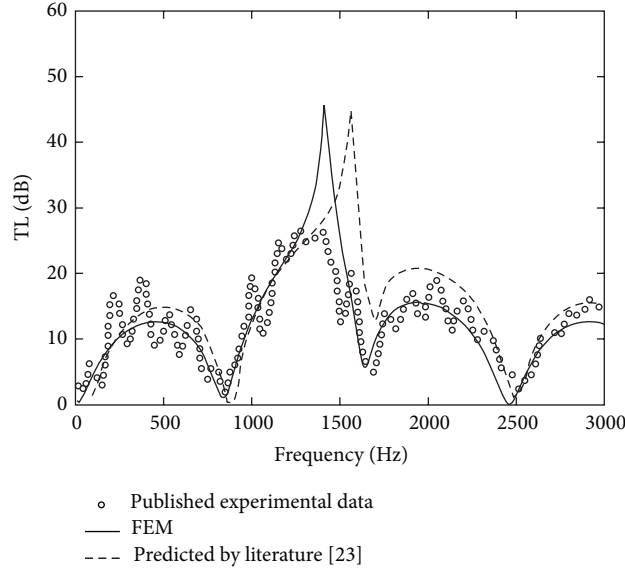


FIGURE 11: Measured and predicted TL for the expansion chamber silencer with inlet flow velocity of $v = 10.2$ m/s.

Substituting (11) and (12) into (6) yields

$$\begin{aligned} \text{TL} &= 10 \log_{10} \left[\frac{(p_{\text{in}} + \rho c)^2}{4p_{\text{out}}^2} \frac{A_{\text{in}}}{A_{\text{out}}} \right] \\ &= 10 \log_{10} \left(\frac{(p_{\text{in}} + \rho c)(\overline{p_{\text{in}} + \rho c})}{4p_{\text{out}}\overline{p_{\text{out}}}} \frac{A_{\text{in}}}{A_{\text{out}}} \right). \end{aligned} \quad (13)$$

It should be noted that the obtained acoustic pressure is in frequency-domain and therefore has a complex value. In this paper, the temperature and density of the medium (air) are $T = 288$ K and $\rho = 1.225$ kg/m³, respectively, and the speed of sound in air is $c = 340$ m/s.

3. Results and Discussion

3.1. Validation of the 3D Numerical Method. Following the calculation steps stated in Section 2.2, CFD steady flow computation is performed first. Figure 5 shows the computed velocity contours on the axial cutting plane of the expansion chamber silencer with extended inlet; it is found that the velocity distribution is uneven. The flow velocity in the inlet and outlet pipes are higher than that in the chamber, and the sudden section area change enhances the turbulent kinetic energy as shown in Figure 6. Figure 7 shows the velocity-vectors for the three straight-through perforated pipe silencers with a mean flow Mach number of $M = 0.1$ or 0.2 . Flow circulations can be observed in the rear part of the chamber, and the velocity in the pipe is much higher than that in the orifices and chamber. Moreover, the magnitude and direction of cross-flow velocity through the perforations are different along the axial direction. In addition, under the action of pressure difference between the chamber and perforated pipe, the gas flows into the chamber through the orifices and then flows back again into the pipe, which enhances the turbulent kinetic energy near the orifices, as shown in

Figure 8. Generally speaking, the flow velocity distributions inside the studied silencers are anisotropic and nonuniform, and the gas flow is accompanied with turbulence.

After importing the mean flow data to the acoustic field by mesh mapping, acoustic response analysis is performed to acquire acoustic pressure at the inlet and outlet as shown in Figures 9 and 10. To validate the accuracy of the 3D numerical method, published experimental and numerical results for the studied silencers are compared with the present predictions.

Figure 11 compares the TL results for the expansion chamber silencer with extended inlet from numerical and experimental methods. The present predictions agree reasonably well with the experimental data in the frequency range of interest. Some deviation from the measurements is observed, for example, near the resonance peak. This discrepancy may be attributed to the fact that (i) the medium viscous effects and wall thickness are neglected in the FEM calculation and (ii) flow noise generated inside the silencer is neglected in the simulation, but the noise is included in the experiments. Furthermore, the present FEM results are compared with the numerical results from literature [23]. One can see that the present FEM yields better results between the predicted TL curves. That is because the method employed in the literature neglects the turbulence inside the silencer and uses the simplified mean flow velocity. In contrast, the present study may acquire more detailed distribution of mean flow through the CFD steady flow computation with the proper turbulence model.

In Figure 12, a comparison between the present predictions and measurements shows a good agreement in general between TL results obtained for the three straight-through perforated pipe silencers studied here. However, it is found that the present predicted TL values are slightly less than those measured. This is because the influence of mean flow on the sound propagation in the silencer can be explained as

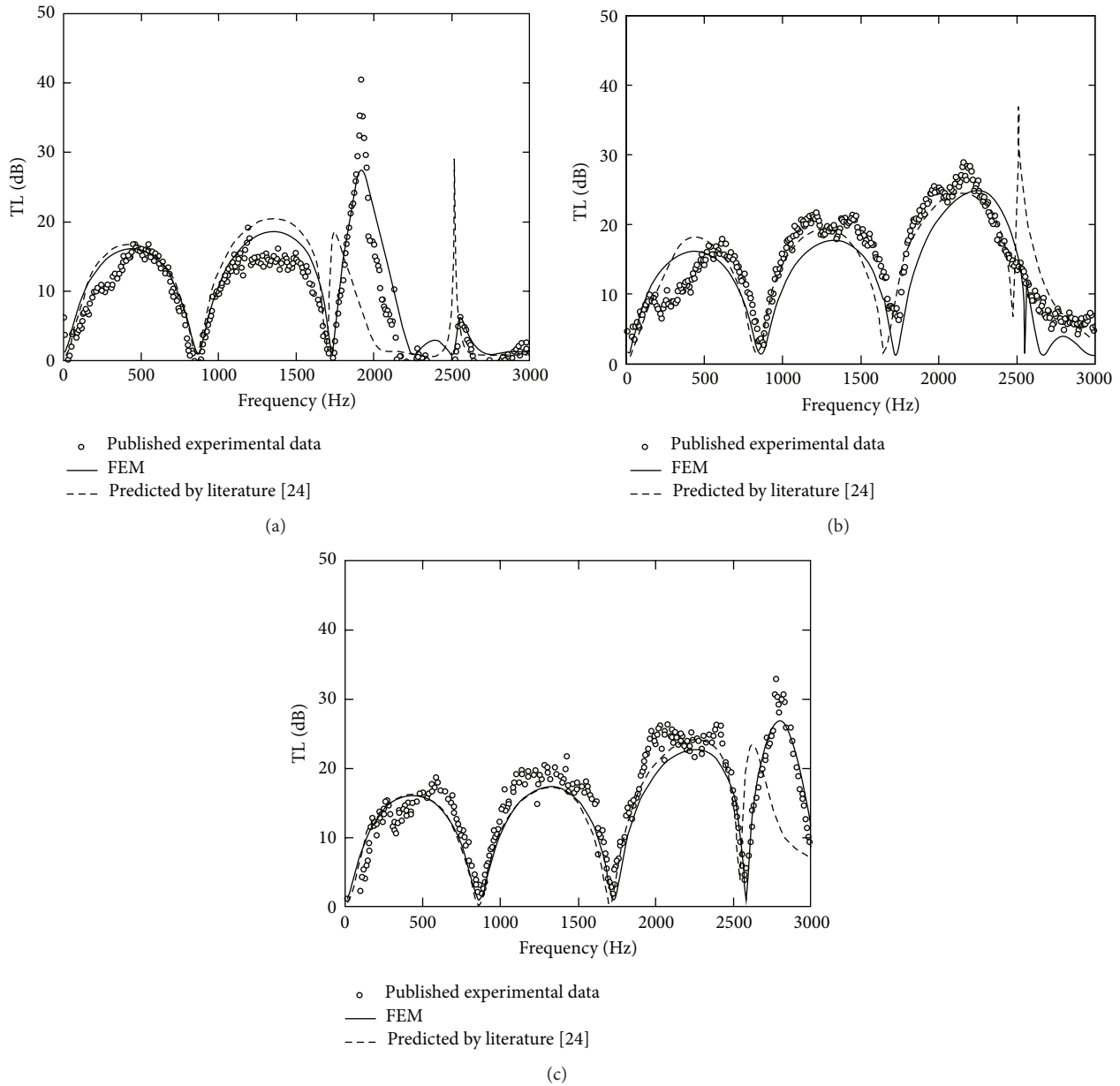


FIGURE 12: Measured and predicted TL for the straight-through perforated pipe silencers: (a) silencer P_1 , $M = 0.1$, (b) silencer P_2 , $M = 0.2$, and (c) silencer P_3 , $M = 0.1$.

the convective and dissipative effects [7], and the convective effect can be considered by importing the decouple mean from an external steady flow computation to the acoustic field, but the dissipative effect of medium viscous (especially in the orifices), which can cause sound energy loss and thus increase TL, is not included in the FEM calculation just like the conventional frequency-domain method. At present, lots of studies, such as [24], mainly focus on applying mathematical modeling of perforate impedance to calculate and analyze the acoustic attenuation performance of perforated pipe silencer. In the absence of mean flow, the acoustic performance of the silence can be accurately predicted with the help of perforate impedance models. However, when

mean flow is present, rigorous mathematical modeling of the mechanisms that determine the perforate impedance is extremely difficult. Therefore, most of current impedance models considering the mean flow effect are empirical. In contrast, although there is a lack of consideration of mean flow dissipative effect on sound propagation in present FEM by decoupling the problems, this method avoids complex mathematical calculation, and it is accessible and easy to use. Furthermore, the predicted results presented are not bad. Therefore, it is valuable for predicting the acoustic attenuation performance of perforated pipe silencer.

At present, with the development of computer performance, the full time-domain CFD method, such as that

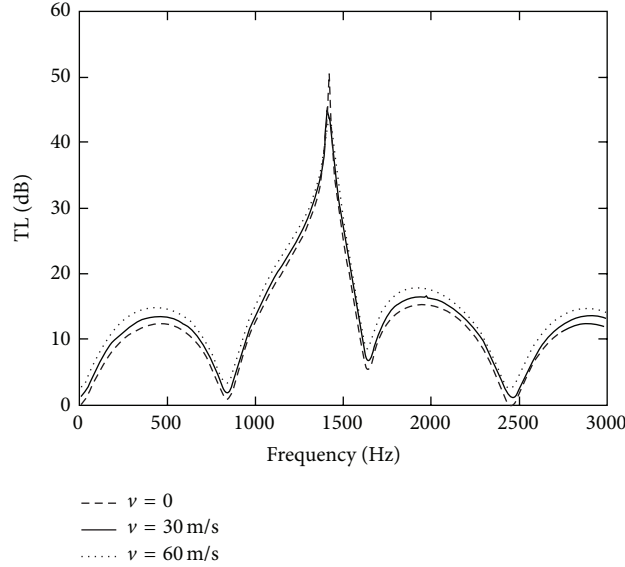


FIGURE 13: Effect of flow velocity on TL of the expansion chamber silencer.

performed in [8], has also attracted the interest of researchers. The main advantage of this method is that the dissipative effect of medium viscous could be better represented. However, compared with the present method, the main problem when using the time-domain CFD method is the CPU time consumed during the transient flow computation due to the fact that long upstream and downstream pipes, typically exceeding 15 times the length of the silencer, are required to capture isolated incident and transmitted signals, and the time window (record length of data) must be long enough to capture the entire pressure signals. Moreover, when mean flow is present, the CFD transient flow computation needs to be run twice (with and without impulse signal). Additionally, it can be seen from [8] that the TL curves calculated by the time-domain CFD method are not smooth and have some sawteeth. This is because the time-domain CFD method is a simulation of the process of an impulse technique [30] for measuring silencer acoustic performance and therefore the predicted TL curves are easy to fluctuate like those obtained from the impulse technique. Middelberg et al. [31] investigated the effect of mesh size on TL obtained from the time-domain CFD method, and they found that, for higher frequencies, the coarse mesh would influence the accuracy of solution due to the inability of the mesh to resolve the wavelength with a sufficient number of points and introduced the artificial numerical dissipation. Therefore, the mesh size for the time-domain CFD method should be small enough to avoid high-frequency dissipation. As mentioned in Section 2.1, two different meshes, CFD mesh and acoustic mesh, are used for the solution of the mean flow and acoustic problems when employing present method. Compared with the mesh used in the time-domain CFD method, the requirements of the CFD mesh for the steady flow computation in present method are much reduced [32], but it should be finer than the acoustic mesh.

3.2. Effect of Mean Flow on Silencer Acoustic Attenuation Performance. Two main effects of mean flow on silencer acoustic performance can be distinguished: one is to affect the sound propagation in the silencer (stated in Section 3.1). The other is to induce aerodynamic noise due to turbulence. In silencers the typical mean flow Mach number is below 0.3 [33], and the aerodynamic noise is considered to be weak. Therefore, the aerodynamic noise is neglected in this work.

Figure 13 shows that the predicted TL curves of the expansion chamber silencer with the flow velocity varied between 0 m/s and 60 m/s. It is observed that the shape of TL curve with mean flow is much similar to that without mean flow. The presence of mean flow increases the TL at most frequencies and decreases the resonance peak, and TL increases further as flow velocities increase. Figure 14 shows the effect of mean flow on TL of the straight-through perforated pipe silencers with different flow velocities. It can be seen from these pictures that the mean flow has little influence on the acoustic attenuation in the plane wave range and leads to complex variation of TL curves in the non-plane wave. Overall, except that the presence of mean flow remarkably decreases resonance peak, the acoustic attenuation performance of the straight-through perforated pipe silencers increases at most frequencies as flow velocity is increased, especially at higher frequencies.

4. Conclusions

In this paper, a 3D numerical method is employed to investigate the acoustic attenuation performance of a circular expansion chamber silencer with extended inlet and three straight-through perforated pipe silencers in the presence of mean flow. By decoupling the problem, the linear acoustics are away from the mean flow computation. CFD and FEM

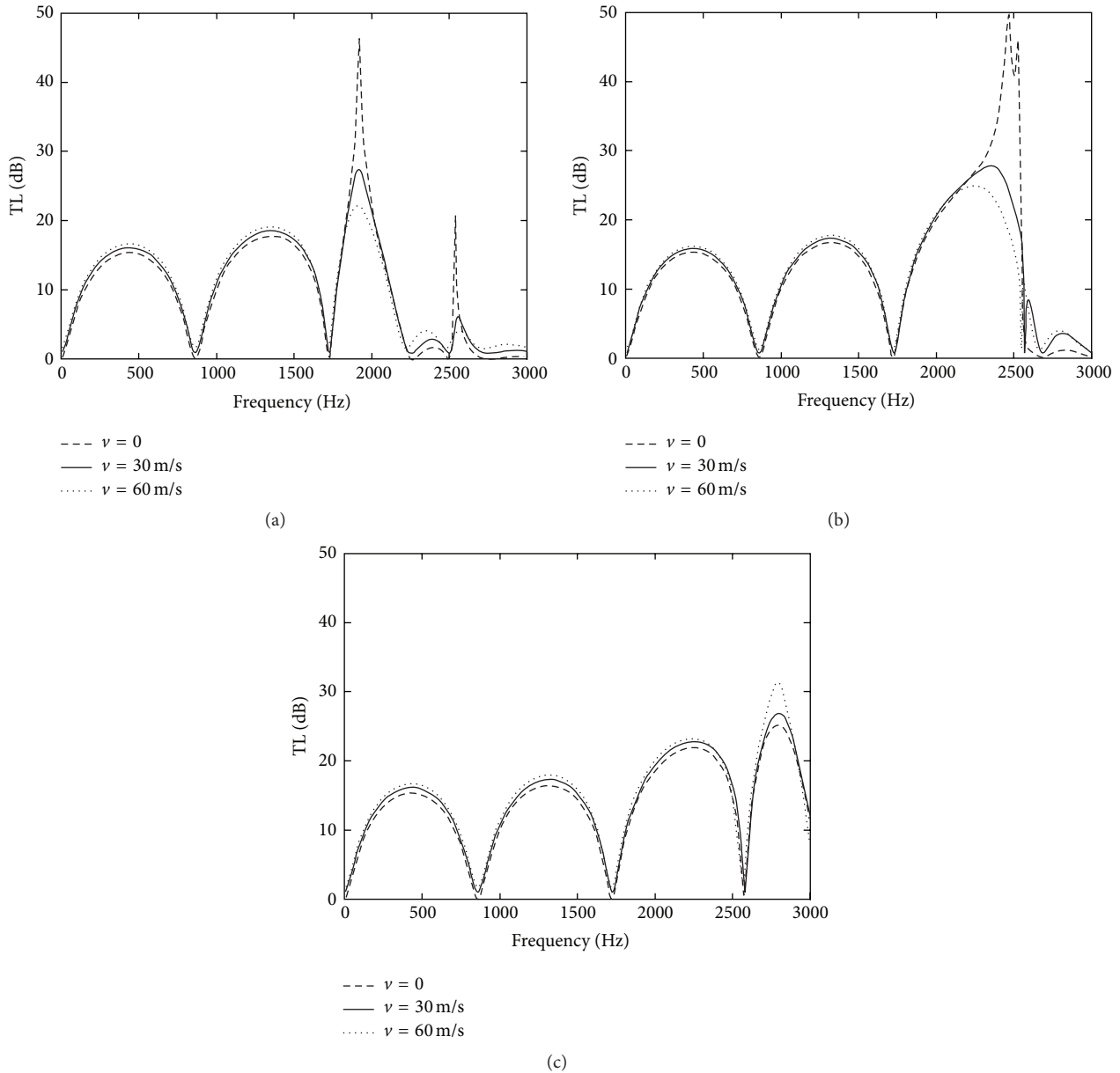


FIGURE 14: Effect of flow velocity on TL of the straight-through perforated pipe silencers: (a) silencer P_1 , (b) silencer P_2 , and (c) silencer P_3 .

are employed to perform the steady flow computation and acoustic response analysis, respectively. The data transfer is accomplished by mesh mapping. A comparison between present results and previously published experimental and numerical results indicates that the present 3D numerical method is capable of delivering reasonable predictions. The major advantage of present method is that it is accessible and easy to use and avoids complex mathematical calculation with the help of simulation software, especially for the perforated pipe silencer, while the major drawback of this method lies in the considerable computational effort and cost that are required to acquire a complete and accurate solution in the 3D calculations.

Furthermore, the TL of studied silencers with different flow velocities is calculated. It is concluded that the presence of mean flow decreases the resonance peak and increases the acoustic attenuation at most frequencies for the expansion chamber silencer. For the straight-through perforated pipe silencer, mean flow has little influence on the acoustic attenuation in the plane wave range and remarkably decreases the resonance peak and increases the acoustic attenuation at higher frequencies.

Conflict of Interests

The authors declare that there is no conflict of interests with regard to this study and the publication of this paper.

Acknowledgments

The authors are grateful for the grants from National Natural Science Foundation of China (51275082, 11272273), Fundamental Research Fund of Central Universities (N130403009), Research Fund for Doctoral Program of Higher Education (20100042110013), and Program for Liaoning Innovative Research Team in University (LT2014006).

References

- [1] M. G. Prasad and M. J. Crocker, "Insertion loss studies on models of automotive exhaust systems," *Journal of the Acoustical Society of America*, vol. 70, no. 5, pp. 1339–1344, 1981.
- [2] M. L. Munjal and P. T. Thawani, "On the transfer matrix for a uniform tube with a moving medium," *Journal of Sound and Vibration*, vol. 91, no. 4, pp. 597–599, 1983.
- [3] K. Narayana Rao and M. L. Munjal, "Experimental evaluation of impedance of perforates with grazing flow," *Journal of Sound and Vibration*, vol. 108, no. 2, pp. 283–295, 1986.
- [4] Y. H. Kim, S. H. Kim, B. D. Lim, and Y. K. Kwak, "Experimental study of acoustic characteristics of expansion chamber with mean flows," *KSME Journal*, vol. 2, no. 2, pp. 125–132, 1988.
- [5] Y. Aurégan and M. Leroux, "Failures in the discrete models for flow duct with perforations: an experimental investigation," *Journal of Sound and Vibration*, vol. 265, no. 1, pp. 109–121, 2003.
- [6] A. Broatch, X. Margot, A. Gil, and F. D. Denia, "A CFD approach to the computation of the acoustic response of exhaust mufflers," *Journal of Computational Acoustics*, vol. 13, no. 2, pp. 301–316, 2005.
- [7] Z. L. Ji, H. S. Xu, and Z. X. Kang, "Influence of mean flow on acoustic attenuation performance of straight-through perforated tube reactive silencers and resonators," *Noise Control Engineering Journal*, vol. 58, no. 1, pp. 12–17, 2010.
- [8] C. Liu and Z.-L. Ji, "Computational fluid dynamics-based numerical analysis of acoustic attenuation and flow resistance characteristics of perforated tube silencers," *Journal of Vibration and Acoustics*, vol. 136, no. 2, Article ID 021006, 11 pages, 2014.
- [9] H.-D. Ju, S.-B. Lee, and Y.-B. Park, "Transmission loss estimation of splitter silencer using multi-domain BEM," *Journal of Mechanical Science and Technology*, vol. 21, no. 12, pp. 2073–2081, 2007.
- [10] Z. L. Ji, "Boundary element acoustic analysis of hybrid expansion chamber silencers with perforated facing," *Engineering Analysis with Boundary Elements*, vol. 34, no. 7, pp. 690–696, 2010.
- [11] C. Jiang, T. W. Wu, M. B. Xu, and C. Y. R. Cheng, "BEM modeling of mufflers with diesel particulate filters and catalytic converters," *Noise Control Engineering Journal*, vol. 58, no. 3, pp. 243–250, 2010.
- [12] C. I. J. Young and M. J. Crocker, "Prediction of transmission loss in mufflers by the finite element method," *Journal of the Acoustical Society of America*, vol. 57, no. 1, pp. 144–148, 1975.
- [13] O. Z. Mehdizadeh and M. Paraschivoiu, "A three-dimensional finite element approach for predicting the transmission loss in mufflers and silencers with no mean flow," *Applied Acoustics*, vol. 66, no. 8, pp. 902–918, 2005.
- [14] Z. Kang and Z. Ji, "Acoustic length correction of duct extension into a cylindrical chamber," *Journal of Sound and Vibration*, vol. 310, no. 4-5, pp. 782–791, 2008.
- [15] Y. S. Ge, H. B. Zhang, Y. R. Zhang, J. W. Tan, X. M. Zhang, and X. K. Han, "An analysis on 3D acoustic performance of automotive exhaust muffler," *Automotive Engineering*, vol. 28, no. 1, pp. 51–55, 2006 (Chinese).
- [16] P. Chaitanya and M. L. Munjal, "Effect of wall thickness on the end corrections of the extended inlet and outlet of a double-tuned expansion chamber," *Applied Acoustics*, vol. 72, no. 1, pp. 65–70, 2011.
- [17] J. Fu, W. Chen, Y. Tang, W. H. Yuan, G. M. Li, and Y. Li, "Modification of exhaust muffler of a diesel engine based on finite element method acoustic analysis," *Advances in Mechanical Engineering*, vol. 7, no. 4, 11 pages, 2015.
- [18] K. S. Peat, "Evaluation of four-pole parameters for ducts with flow by the finite element method," *Journal of Sound and Vibration*, vol. 84, no. 3, pp. 389–395, 1982.
- [19] X. R. Wang and Z. L. Ji, "Boundary element analysis of four-pole parameters and transmission loss of silencers with flow," *Chinese Journal of Computational Physics*, vol. 24, no. 6, pp. 717–724, 2007 (Chinese).
- [20] N. Gil-Negrete, A. Rivas, and J. Viñolas, "Predicting the dynamic behaviour of hydrobushings," *Shock and Vibration*, vol. 12, no. 2, pp. 91–107, 2005.
- [21] S. N. Panigrahi and M. L. Munjal, "Backpressure considerations in designing of cross flow perforated-element reactive silencers," *Noise Control Engineering Journal*, vol. 55, no. 6, pp. 504–515, 2007.
- [22] A. J. Torregrosa, P. Fajardo, A. Gil, and R. Navarro, "Development of non-reflecting boundary condition for application in 3D computational fluid dynamics codes," *Engineering Applications of Computational Fluid Mechanics*, vol. 6, no. 3, pp. 447–460, 2012.
- [23] C.-N. Wang, "A boundary element analysis for simple expansion silencers with mean flow," *Journal of the Chinese Institute of Engineers*, vol. 23, no. 4, pp. 529–536, 2000.
- [24] S.-H. Lee and J.-G. Ih, "Empirical model of the acoustic impedance of a circular orifice in grazing mean flow," *Journal of the Acoustical Society of America*, vol. 114, no. 1, pp. 98–113, 2003.
- [25] F. L. Zhan and J. W. Xu, *Virtual.Lab Acoustics Simulation from Entry to Master*, Northwestern Polytechnical University Press, Xian, China, 2013 (Chinese).
- [26] ANSYS Inc, *ANSYS FLUENT 14.5 in Workbench User's Guide*, ANSYS Inc, New York, NY, USA, 2012.
- [27] LMS International NV, *LMS Virtual.Lab Online Help11-SL2*, LMS International N. V., Leuven, Belgium, 2013.
- [28] C. Liu, Z. L. Ji, and Z. Fang, "Numerical analysis of acoustic attenuation and flow resistance characteristics of double expansion chamber silencers," *Noise Control Engineering Journal*, vol. 61, no. 5, pp. 487–499, 2013.
- [29] M. L. Munjal, *Acoustic of Ducts and Mufflers*, Wiley, New York, NY, USA, 2014.
- [30] R. Singh and T. Katra, "Development of an impulse technique for measurement of muffler characteristics," *Journal of Sound and Vibration*, vol. 56, no. 2, pp. 279–298, 1978.
- [31] J. M. Middelberg, T. J. Barber, S. S. Leong, K. P. Byrne, and E. Leonardi, "CFD analysis of the acoustic and mean flow performance of simple expansion chamber mufflers," in *Proceedings of the ASME International Mechanical Engineering Congress and Exposition*, pp. 151–156, Anaheim, Calif, USA, November 2004.

- [32] B. K. Gardner, A. Mejdi, F. Mendonca, and D. Copley, "Using CFD flow fields to inform acoustic finite element models of complex mufflers with thermal and flow effects," in *Proceedings of the 44th International Congress and Exposition on Noise Control Engineering*, Paper 15-665, San Francisco, Calif, USA, August 2015.
- [33] E. Dokumaci, "Effect of sheared grazing mean flow on acoustic transmission in perforated pipe mufflers," *Journal of Sound and Vibration*, vol. 283, no. 3-5, pp. 645-663, 2005.



Hindawi

Submit your manuscripts at
<http://www.hindawi.com>

